ELSEVIER

Polymer 44 (2003) 2379–2384

polymer

www.elsevier.com/locate/polymer

Pattern formation in polymer films under the mask

Juan Peng, Yanchun Han*, Yuming Yang, Binyao Li

State Key Laboratory of Polymer Physics and Chemistry, Changchun Institute of Applied Chemistry, Chinese Academy of Sciences, Changchun 130022, People's Republic of China

Received 13 September 2002; received in revised form 30 December 2002; accepted 3 January 2003

Abstract

This paper presents a straightforward method for patterning thin films of polymers, i.e. a prepatterned mask is used to induce self-assembly of polymers and the resulting pattern is the same as the lateral structures in the mask on a submicrometre length scale. The patterns can be formed at above $T_g + 30$ °C in a short time and the external electric field is not crucial. Electrostatic force is assumed to be the driving force for the pattern transfer. Viscous fingering and novel stress-relief lateral morphology induced under the featureless mask are also observed and the formation mechanisms are discussed.

Keywords: Patterning; Polymer film; Electrostatic instability

1. Introduction

Patterned thin polymer films have a wide range of applications, for example, in preventing etching [1], in molecular electronics [2–4], in optical devices [5–7], in biological [8] and chemical sensors [9–11], and in tissue engineering [12]. Therefore, there is an increasing need to develop low-cost and high throughput methods for patterning thin polymer films. Some techniques, for example, conventional lithography (photolithography, extreme ultraviolet lithography, etc.), non-conventional lithography (embossing [13,14], soft lithography [7,15], etc.), have been used to pattern the thin polymer films. Although photolithography is a widely used microlithographic technique in microfabrication, it has a number of disadvantages. It is relatively expensive and can only directly applicable to limited photosensitive materials [16]. It almost, cannot control the properties of the patterned surfaces. It has the optical diffraction limit thus cannot pattern features down to 100 nm. Soft lithography is a newly developing technique including microcontact printing [17], microtransfer molding [18], micromolding in capillaries [15], etc. These techniques and embossing, which are based on the printing of self-assembled monolayers (SAMs) and molding of organic polymers, have a common feature of using a patterned elastomer as the stamp or mold to produce microstructures [19]. Soft lithography circumvents the diffraction limitation of photolithography and thus offers a new strategy for microfabrication with feature size ≤ 100 nm. However, soft lithography is still in an early stage of technical development. There are a number of issues that remain to be solved before soft lithography can compete with photolithography in the core application of microfabrication, including pattern distortion caused by elastomer deformation and uneasy to get high resolution registration, etc. Furthermore, phase separation of polymer blends and diblock copolymers [20,21], and dewetting of thin polymer films [22,23] are also developed to pattern thin polymer films. However, scientists never stop to pursue new patterning methods for thin polymer films. Recently, an intriguing pattern transfer technique named lithographically induced self-assembly (LISA) was discovered by Chou and co-workers [24–26]. Their experiment showed that when a mask with protruded patterns was placed a certain distance above a flat polymer melt (polymethylmethacrylate (PMMA)), the polymer would be attracted to the below of mask protrusions. Thus the patterns had a lateral dimension identical to that of the mask protrusions. Similar observations on polystyrene were made by Schäffer et al. [27], however, under the condition that external

* Corresponding author. Tel.: 86-431-5262175; fax: 86-431-5262126.
E-mail address: ychan@ciac.jl.cn (Y. Han).

0032-3861/03/$ - see front matter © 2003 Elsevier Science Ltd. All rights reserved.
doi:10.1016/S0032-3861(03)00041-7

electric field was applied between the mask and the polymer melt. Their fascinating results showed that using a mask to induce and pattern polymer films is a straightforward, feasible technique to fabricate sub-micrometer and possibly nanometer structures.

In this paper, we have carried out a series of experiments under different conditions to optimize the process of LISA. Both polymethylmethacrylate (PMMA) and polystyrene (PS) films are perfectly patterned by LISA with the lateral length scales down to 500 nm. The mechanism of pattern transfer has been discussed in detail. In addition, two phenomena of viscous fingering and novel stress-relief lateral morphology are observed during the process of LISA under the flat mask and their formation mechanisms are discussed.

2. Experimental

Polymers used were polymethylmethacrylate **1** ($M_w = 15,000$, Aldrich), polystyrene **2** ($M_w = 29,300$, Aldrich). The polymer toluene solutions (1 wt%) were spin-cast on the pre-cleaned silicon wafers followed by baking at 80 °C to drive off the solvent. The thickness of both the PMMA and PS films was about 40 nm measured by an ellipsometry (AUEL-III, Xi'an, China). In the experimental process, a polymer film was placed on a plate. Facing it, a mask was mounted a certain distance from the film by the spacer. A pressure of about 1 MPa was applied by sandwiching them between two press plates. The system was then heated for times ranging from 5 min to 4.5 h at temperatures of 130–170 °C. After the sample was cooled, the system was disassembled and the morphology of the polymer film was observed by optical microscopy (XJX-2, Nanjing, China) and atomic force microscopy (SPI3800N, Seiko Instruments Inc., Japan). Two kinds of masks were used in the experiment. One of the mask used had grating features with periods of 700 nm and the height of about 1.3 μm (Fig. 1), which was fabricated by UV lithography. Thin rails of titanium oxide were evaporated on the mask as the spacer with the height of 200 nm. The other kind of mask was fabricated by directly evaporating 110 nm high aluminium pillars as the spacer through a shadow mask on a highly polished silicon wafer. To avoid the sticking problems, a fluorinated silane surfactant was pre-coated on the mask.

3. Results and discussion

3.1. Pattern formation in polymer films under stripe patterned mask

Heated the set-up in Fig. 1 to 130 °C for 5 min, then cooled it to room temperature, after the upper mask was taken off, some patches of the PMMA film were observed to display iridescent colors owing to the interference of light. By the use of atomic force microscopy performed in tapping mode, highly ordered, straight stripes can be seen clearly (Fig. 2b), which had lateral width identical to that of stripes on the mask (The striped-pattern on mask is shown in Fig. 2a. The width of the stripes and the grooves is 500 and 200 nm, respectively). The cross-sectional image in Fig. 2b reveals a stripe height of 73 nm and the rounded top corners indicate the formed stripes have not reached the mask protruding pattern. PS film also shows similar stripes (Fig. 2c) without any external electric field on the contrary to the results of Schäffer et al. [27]. Compared the images of the mask and polymer films, the quality of the formed structures is nearly perfect and the pattern can cover more than 100×100 μm^2 area.

To follow up the pattern formation process during LISA, we performed the experiments under different conditions. First, the heating temperature was fixed at 130 °C with the heating time ranging from 5 min to 4.5 h. We found that it was hardly to observe the evolution process of the pattern formation of PMMA films. No distinct differences were found when heating time varied from 5 min to 4.5 h and 5 min was enough to induce the patterns in polymer film under the mask. It meant that the process was very fast from an initial featureless flat film developing to the final stripe morphology. Temperature dependent studies were also investigated during LISA. PS films were heated at 130, 150, 170 °C for 5 min, respectively. Each film was then observed by the microscopy. The patterns of stripes all appeared in the three films without much distinction. All these results showed that the pattern formation happened very fast at the temperature above $T_g + 30$ °C.

To further confirm the effect of external electric field on the LISA, two PS films were used for comparison of which one was applied a small voltage (30 V) and the other without applying voltage. Other experimental conditions were identical with the heating time of 5 min and the temperature of 130 °C. To assure the good electric conductivity, the silicon wafers used were highly doped with phosphorus and the backside of them was coated with a

Fig. 1. Schematic illustration of the experimental set-up. The electrostatic force generates and further amplifies instability at the polymer-air interface. When a patterned top mask is used, the instability is focused under the protrusions of mask and caused the pattern formation.

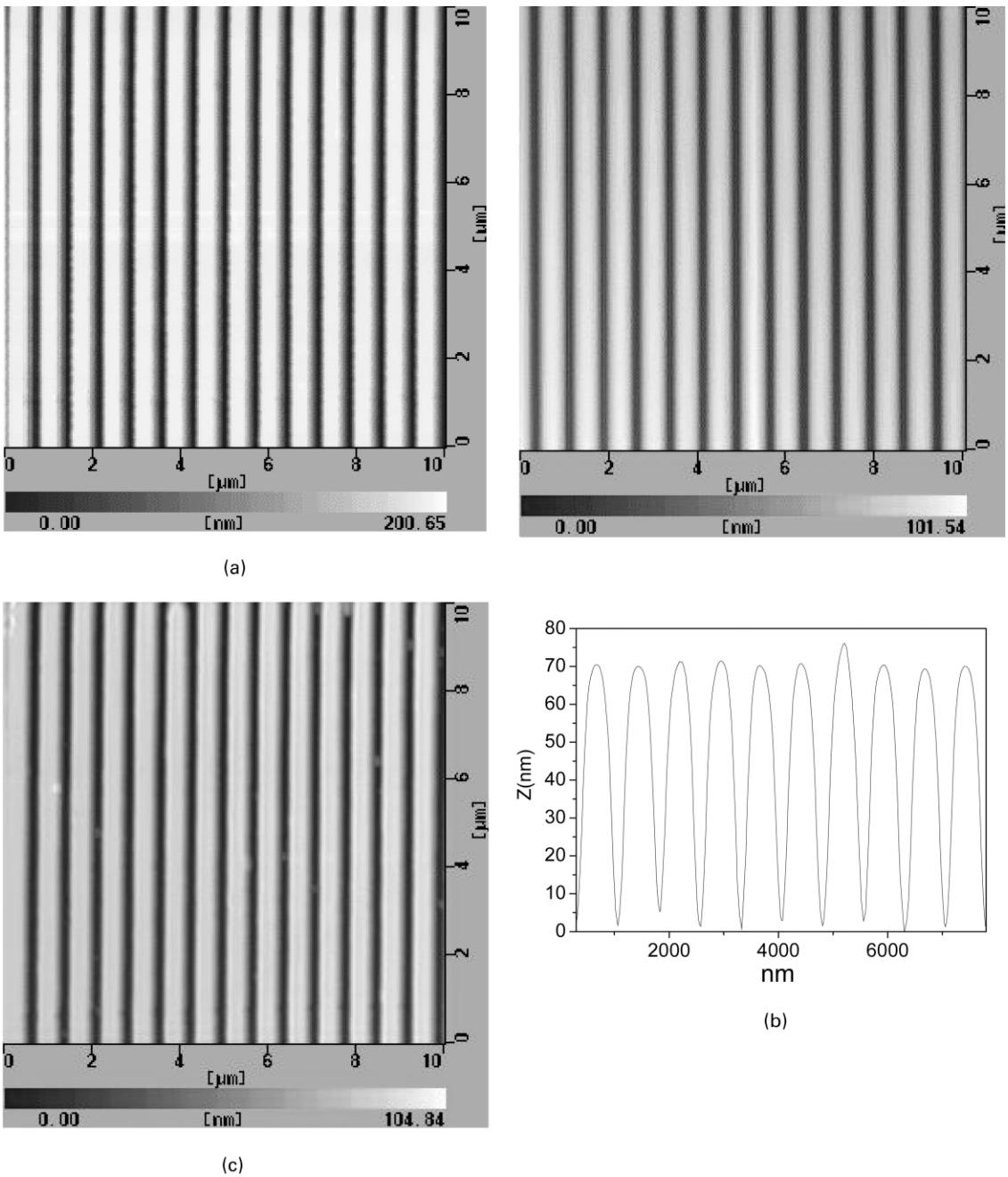

Fig. 2. AFM images of the stripes pattern. (a) The stripes pattern on the mask. It shows the width of the stripes and the grooves is 500 and 200 nm, respectively. The height of stripes is about 1.3 μm but the resolution is limited due to the large size of AFM tip. (b) The pattern of stripes formed in PMMA film. Stripes with the width of 500 nm and a periodicity of 700 nm are produced, which indicates a perfect transfer from the mask to the polymer film. The cross-sectional image reveals a height of 73 nm. (c) The same pattern of stripe formed in PS film.

thin aluminium layer. We investigated the morphology of the two PS films using optical microscopy and found that the stripe patterns appeared in both films with the same lateral size further measured by AFM. It showed that external electric field was not necessary to the formation of patterns during LISA. With that a third PS film was heated under the same condition while short-circuiting the top and bottom plates to eliminate the static charge accumulation. In contrast, such straight stripes were not observed. Therefore, it can be concluded that the existence of static charge is essential for the formation of ordered stripes.

3.2. Mechanisms of pattern transfer

Theory and models have been proposed in the literatures to explain this phenomenon. Schäffer and co-workers believed that it was caused by the dielectric media experiences a force in an electric field gradient [27–29].

Strong field gradients can produce forces that overcome the surface tension in thin liquid films, inducing the electrohydrodynamic (EHD) instability. The instability is focused towards the downward protruding patterns of the top mask. Therefore, the liquid polymer is drawn towards these protrusions, forming positive replica. Chou et al. proposed a model called the image charge-induced electrohydrodynamic-instability (ICE) model to explain the intriguing phenomenon [25]. The model assumed that the electrostatic force is the driving force despite under no electric field. When heating the polymer above its glass transition temperature, the charges increase significantly and induce the same quantity of image charges in the upper mask. The interaction between the charges and the image charges caused the instability in film and the formation of patterns thereafter. Some other groups gave such as 'leaky dielectric model' [30] and theories [31] about 'the minimum free energy and phase refining' to explain the phenomenon theoretically.

Here, we propose a simple mechanism of pattern formation from another point of view. Since the electrostatic force is assumed as the driving force, the exact sources of the electrostatic charge must be clarified. Because the film used is very thin, certainly there exist defects that are more or less conducting dust particles or pinholes at which electron exchanges cladding the film may take place [32]. This leads to an electric potential difference and thus the electric field is built up across the film. Comparing the small gap between the mask and the polymer, the potential between dissimilar materials can produce relatively strong electric field. Even for apolar PS liquid film, the large dielectric contrast between PS and air plays a role. After the polymer is heated above its T_g, it begins to flow as a viscous liquid. The polymer experiences surface tension and gravity, which act as stabilizing factors and the electrostatic force which is the destabilizing influence. The overall pressure at the interface can be written as [28]

$$p = p_0 - \gamma \frac{\partial^2 h}{\partial x^2} + p_{el}(h) + p_{dis}(h) \quad (1)$$

where p_0 is the atmospheric pressure, γ is the surface tension, and h is the film thickness. The second, the third and the fourth term represent the Laplace pressure, electrostatic pressure and the disjoining pressure in the film, respectively. Once the electrostatic pressure exceeds a critical value, the interface will be unstable resulting sinusoidal profile. Such instability can be further amplified leading rearrangement of the configuration energetically favored. Since the vertical configurations have the lower electrostatic free energy than lamellar configurations [31], the electrostatic force drives the polymer melt to grow upward at a cost of adding some interface energy. Such instability is focused in the direction of the highest external field. Because the electrostatic forces are strongest for smallest distance, the protruded patterns on the mask guide the growth and finally transfer themselves to the polymer film. Due to mass conservation, such growth almost depletes surrounding matters. To explore the influence of the height of spacer, another mask was used which had the same grating features with 400 nm high silicon oxide as the spacer. Similar stripe pattern is obtained with a different height of 160 nm. We can safely assume that on further increasing the spacer height to a certain extent, higher stripes also appear. Once the critical value is exceeded, the electrostatic force is too small to overcome the surface tension and the gravity of polymers and thus no stripes will form.

3.3. Formation of other patterns under featureless mask

When placing a featureless mask at a certain distance above the PMMA film, we observed two beautiful patterns induced under the flat mask. The two patterns can coexist on the same sample while their formation mechanisms are different. One is the viscous fingering (Fig. 3a and b) belonging to the fractal geometry. Fractals are far-from-equilibrium growth phenomena that are common in many fields of science and technology, such as dendritic crystallization, electrodeposition, viscous fingering, and dielectric breakdown [33], etc. When a fluid pushes a more viscous fluid in a very narrow gap between parallel plates, the interface between the two fluids develops an instability leading to the formation of fingerlike patterns called viscous fingers [34–36]. Trapped air underneath the flat mask is the less viscous fluid to drive the polymer melt. This geometry is called a Hele–Shaw cell [37]. Fig. 3a and b show two types of fingers. The physical source of this instability lies in the geometry of the moving interface [38]. Disturbances cause a local protrusion in the spreading front and the thickened portions spread faster than adjacent thinner regions, thereby destabilizing an initially uniform front [39]. In both experiments and simulations, a dimensionless parameter called 'surface tension parameter' was introduced as a control parameter, namely,

$$d_0 = (\pi^2/3)(b^2/W^2)(T/\mu U) \quad (2)$$

where U is the fluid velocity, b, W, T and μ are the plate spacing, the width of the rectangular cell, the surface tension and the fluid viscosity, respectively. According to the simulations of Bensimon [38], motion is towards the top of finger. At the onset of instability, the finger becomes asymmetric. When d_0 is smaller corresponding to higher fluid velocity, the tip of the finger splits and for the even smaller values of d_0, the finger evolves into a highly branched and apparently dendritic structure. The tallest fingers get ahead and leave the smaller ones well behind, like the structure of Fig. 3b. Though quantitative measurements about viscous fingering in the experiment is difficult, it is assumed that when decreasing the distance b between the two plates corresponding to increasing the trapped air pressure, the fingers will split with more and more reduced curvature radius of the tips.

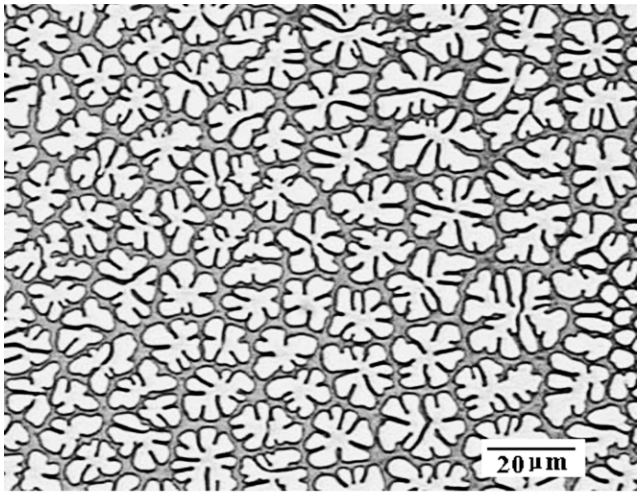

(a)

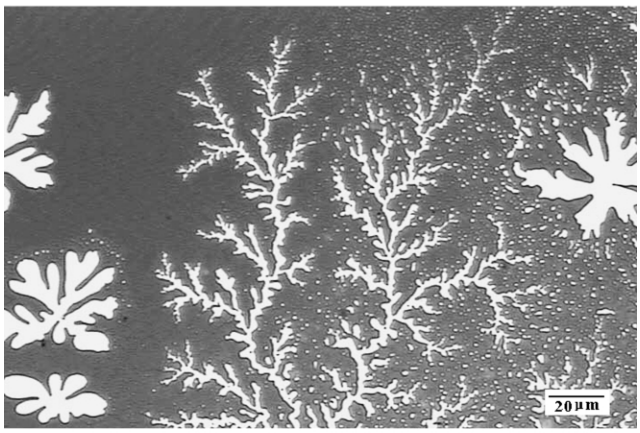

(b)

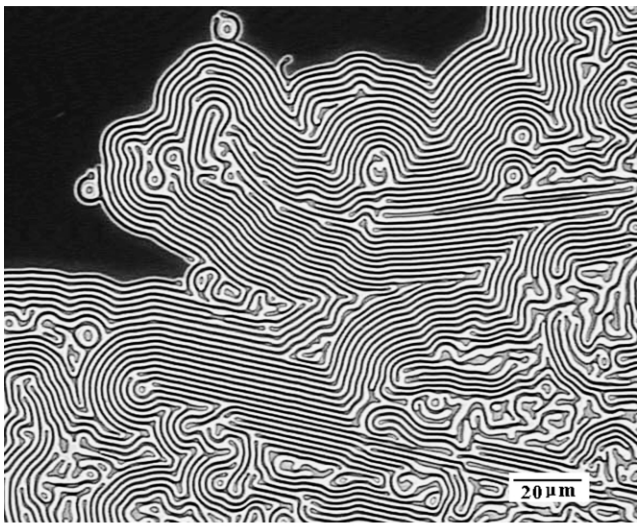

(c)

Fig. 3. Optical micrographs of other phenomena induced by the flat mask during LISA. The device was heated at 135 °C for 3 h. (a and b) Two types of viscous fingers appear in the same sample, in which b appears branched and dendritic. (c) A novel lateral morphology similar to that observed in polymer blend films. Well-defined, parallel stripes are produced in mechanically confined polymer films by compressive stress.

Another aesthetic pattern observed is a novel lateral morphology shown in Fig. 3c. It can be seen that most of the areas are well-defined, parallel stripes with identical inter-stripe spacing. The alternating light and dark regions indicate the orientation of the lamella is perpendicular to the substrate. In the middle right hand, there is an area of meandering pattern of lines and spiral morphology. It is noteworthy that such parallel stripes pattern could not be obtained by heating the PMMA film in the absence of upper mask. Therefore, it is believed that the upper mask provides some degree of mechanical confinement on the film and promotes the pattern formation. Since the spacer used here is conductive, the stripes formation is not due to the electrostatic instability. In addition, the polymer films used are very thin, convective instabilities like the Rayleigh–Bérnard [40] or Marargoni–Bérnard [41] effect are ruled out. We attribute this effect to stress-relief lateral morphology in mechanically confined polymer films. The role of the upper mask is in creating a stress that is compressive upon heating which is opposed by the tensile stress. Once the compressive stress exceeds the tensile stress, the films begin to buckle at wavelength that depends on the magnitude of the stress and the film thickness, etc. Furthermore, the surface stress is anisotropic, such formed stripes will select certain orientations to minimize the free energy [42].

4. Conclusions

We have shown the high-quality stripes with lateral length scales down to 500 nm in the polymer films can be readily formed by LISA. The beauty of this approach is its simplicity and high resolution. The extension to pattern arbitrary feature with lateral length scales down to 100 nm which seems feasible dependent on the mask itself. Also, this method can be extended to pattern other polymers and organic light-emitting materials. LISA can be formed over a range of experimental parameters and external electric field is proved to be unnecessary for it. The electrostatic force is assumed to be the driving force to pull polymers upward energetically favored. Two aesthetic phenomena are also observed under the flat mask during LISA which are viscous fingering driven by the viscosity difference and novel lateral morphology induced by stress relief.

Acknowledgements

This work is subsidized by the National Natural Science Foundation of China for General (20023003, 20274050) and Major (50290090) Program and National Science Fund for Distinguished Young Scholars of China (50125311), and the Ministry of Science and Technology of China for Special Pro-funds for Major State Basic Research Projects (2002CCAD4000). The authors also thank for the Chinese

Academy of Sciences for Distinguished Talents Program and Intellectual Innovations Project (KGCX2-205-03), and Jilin Province for Distinguished Young Scholars Fund (20010101). The authors are also grateful to Prof. Lingjie Guo for preparing the mask and helpful discussion.

References

[1] Xia Y, Mrksich M, Kim E, Whitesides GM. J Am Chem Soc 1995; 117:9576.
[2] Burn PL, Kraft A, Baigent DR, Bradley DDC, Brown AR, Friend RH, Gymer RW, Holmes AB, Jackson RW. J Am Chem Soc 1993;115: 10117.
[3] Dai L, Griesser HJ, Hong X, Mau AWH, Spurling TH, Yang Y, White JW. Macromolecules 1996;29:282.
[4] Nishizawa M, Shibuya M, Sawaguchi T, Matsue T, Uchida I. J Phys Chem 1991;95:9042.
[5] Burn PL, Holmes AB, Kraft A, Bradley DDC, Brown AR, Friend RH, Gymer RW. Nature 1992;356:47.
[6] Healey BG, Foran SE, Walt DR. Science 1995;269:1078.
[7] Xia Y, Kim E, Zhao XM, Rogers JA, Prentiss M, Whitesides GM. Science 1996;273:347.
[8] Knoll W, Matsuzawa M, Offenhausser A, Ruhe J. Isr J Chem 1996;36: 357.
[9] Bruening ML, Zhou Y, Aguilar G, Agee R, Bergbreiter DE, Crooks RM. Langmuir 1997;13:770.
[10] Liu Y, Zhao M, Beigbreiter DE, Crooks RM. J Am Chem Soc 1997; 119:8720.
[11] Wells M, Crooks RM. J Am Chem Soc 1996;118:3988.
[12] Langer R, Vacanti JP. Science 1993;260:920.
[13] Chou SY, Krauss PR, Renstrom PJ. Science 1996;272:85.
[14] Chou SY, Krauss PR, Renstrom PJ. Appl Phys Lett 1995;67:3114.
[15] Kim E, Xia Y, Whitesides GM. Nature 1995;376:581.
[16] Qin D, Xia Y, Rogers JA, Jackman RJ, Zhao X, Whitesides GM. Top Curr Chem 1998;194:1.
[17] Jackman R, Wilbur J, Whitesides GM. Science 1995;269:664.
[18] Zhao X, Xia Y, Whitesides GM. Adv Mater 1996;8:837.
[19] Xia Y, Whitesides GM. Annu Rev Mater Sci 1998;28:153.
[20] Böltau M, Walheim S, Mlynek J, Krausch G, Steiner U. Nature 1998; 391:887.
[21] Li X, Han YC, An LJ. Langmuir 2002;18:5293.
[22] Higgins AM, Jones RAL. Nature 2000;404:476.
[23] Lu G, Li W, Yao J, Zhang G, Yang B, Shen J. Adv Mater 2002;14: 1049.
[24] Chou SY, Zhuang L, Guo L. Appl Phys Lett 1999;75:1004.
[25] Chou SY, Zhuang L. J Vac Sci Technol B 1999;17:3197.
[26] Deshpande P, Sun X, Chou SY. Appl Phys Lett 2001;79:1688.
[27] Schäffer E, Thurn-Albrecht T, Russell TP, Steiner U. Nature 2000; 403:874.
[28] Schäffer E, Thurn-Albrecht T, Russell TP, Steiner U. Europhys Lett 2001;53:518.
[29] Lin Z, Kerle T, Russell TP, Schäffer E, Steiner U. Macromolecules 2002;35:3971.
[30] Pease III LF, Russel WB. J Non-Newtonian Fluid Mech 2002;102: 233.
[31] Suo Z, Liang J. Appl Phys Lett 2001;78:3971.
[32] Herminghaus S. Phys Rev Lett 1999;83:2359.
[33] Vicsek T. Fractal growth phenomena. Singapore: World Scientific Publishing Co. Pte. Ltd; 1989. pp. 297–324.
[34] Lindner A, Coussot P, Bonn D. Phys Rev Lett 2000;85:314.
[35] Saffman PG, Taylor GI. Proc R. Soc London A 1958;245:312.
[36] Bonn D, Kellay H, Amar MB. Meunier J Phys Rev Lett 1995;75:2132.
[37] Hele-Shaw HJS. Nature 1898;58:34.
[38] Bensimon D, Kadanoff LP, Liang S, Shraiman BI, Tang C. Rev Mod Phys 1986;58:977.
[39] Kataoka DE, Troian SM. Nature 1999;402:794.
[40] Bodenschatz E, Pesch W, Ahlers G. Annu Rev Fluid Mech 2000;32: 709.
[41] Vanhook SJ, Schatz MF, Swift JB, Mccormick WD. J Fluid Mech 1997;345:45.
[42] Gao YF, Lu W, Suo Z. Acta Materialia 2002;50:2297.